Free Radical Biology and Medicine 134 (2019) 394–405

Contents lists available at ScienceDirect

Free Radical Biology and Medicine

journal homepage: www.elsevier.com/locate/freeradbiomed

Heat shock protein B1 is a key mediator of prolactin-induced beta-cell cytoprotection against oxidative stress

Letícia F. Terra[a,b], Rosangela A.M. Wailemann[a], Ancély F. dos Santos[a], Vinicius M. Gomes[a], Railmara P. Silva[a], Anna Laporte[b], Flávia C. Meotti[a], Walter R. Terra[a], Giuseppe Palmisano[c], Stephan Lortz[b,**], Leticia Labriola[a,*]

[a] Departamento de Bioquimica, Instituto de Quimica, Universidade de São Paulo (USP), Av. Prof. Lineu Prestes 748, 05508-000 Sao Paulo, Brazil
[b] Institute of Clinical Biochemistry, Hannover Medical School (MHH), Carl-Neuberg-Straße, 1, 30625, Hannover, Germany
[c] Departamento de Parasitologia, Instituto de Ciencias Biomedicas (Edifício II), Universidade de São Paulo (USP), Av. Prof. Lineu Prestes 1374, 05508-000 Sao Paulo, Brazil

ARTICLE INFO

Keywords:
Beta-cell
Diabetes
HSPB1
Prolactin
Oxidative stress
Cytoprotection

ABSTRACT

Maintaining islet cell viability *in vitro*, although challenging, appears to be a strategy for improving the outcome of pancreatic islet transplantation. We have shown that prolactin (PRL) leads to beta-cell cytoprotection against apoptosis, an effect mediated by heat shock protein B1 (HSPB1). Since the role of HSPB1 in beta-cells is still unclear and the hormone concentration used is not compatible with clinical applications because of all the side effects displayed by the hormone in other tissues, we explored the molecular mechanisms by which HSPB1 mediates beta-cell cytoprotection.

Lysates from PRL- and/or cytokine-treated MIN6 beta-cells were subjected to HSPB1 immunoprecipitation followed by identification through mass spectrometry. PRL-treated cells presented an enrichment of several proteins co-precipitating with HSPB1. Of note were oxidative stress resistance-, protein degradation- and carbohydrate metabolism-related proteins.

Wild type, HSPB1 silenced or overexpressing MIN6 cells were exposed to menadione and hydrogen peroxide and analysed for several oxidative stress parameters. HSPB1 knockdown rendered cells more sensitive to oxidative stress and led to a reduced antioxidant capacity, while prolactin induced an HSPB1-mediated cytoprotection against oxidative stress. HSPB1 overexpression, however, led to opposite effects. PRL treatment, HSPB1 silencing or overexpression did not change the expression nor activities of antioxidant enzymes, it also did not lead to a modulation of total glutathione levels nor G6PD expression. However, HSPB1 levels are related to a modulation of GSH/GSSG ratio, G6PD activity and NADPH/NADP $^{+}$ ratio.

We have shown that HSPB1 is important for pro-survival effects against oxidative stress-induced beta-cell death. These results are in accordance with PRL-induced enrichment of HSPB1-interacting proteins related to protection against oxidative stress. Finally, our results outline the need of further studies investigating the importance of HSPB1 for beta-cell viability, since this could lead to the mitigation of beta-cell death through the up-regulation of an endogenous protective pathway.

1. Introduction

Transplantation of pancreatic islets constitutes a promising alternative treatment for type 1 diabetes mellitus, although it is severely limited by the shortage of organ donors. *Ex vivo* maintenance of islet cell mass appears to be an attractive strategy and islet fate in culture is, at least in part, determined by the balance between pro- and anti-apoptotic mediators. Therefore, improvement of islet quality as well as cytoprotection could lead to more viable islets, which, in turn, will increase the success rate of islet transplantation. Previous results from our laboratory have demonstrated a significant beneficial effect of prolactin (PRL) treatment on cell proliferation and secretory function of

* Corresponding author.
** Corresponding author.
E-mail addresses: leterra@iq.usp.br (L.F. Terra), rosangelawailemann@gmail.com (R.A.M. Wailemann), ancely@iq.usp.br (A.F. dos Santos), vinickjp@gmail.com (V.M. Gomes), railmara@iq.usp.br (R.P. Silva), laporte.anna@mh-hannover.de (A. Laporte), flaviam@iq.usp.br (F.C. Meotti), warterra@iq.usp.br (W.R. Terra), palmisano.gp@gmail.com (G. Palmisano), lortz.stephan@mh-hannover.de (S. Lortz), labriola@iq.usp.br (L. Labriola).

https://doi.org/10.1016/j.freeradbiomed.2019.01.023
Received 17 August 2018; Received in revised form 15 January 2019; Accepted 20 January 2019
Available online 27 January 2019
0891-5849/ © 2019 Elsevier Inc. All rights reserved.

cultured human islets [1]. Moreover, the proportion of apoptotic human beta-cells after serum starvation and cytokine treatment was significantly lower in the presence of PRL [2]. These results also suggest that the improvement of cell survival involves the inhibition of cell death pathways controlled by BCL2 family members [2].

Recent results from our lab showed that in beta-cells, PRL leads to the upregulation of heat shock protein B1 (HSPB1), a protein from the family of the small heat shock proteins (sHSP) [3]. In fact, silencing its expression in beta-cells by shRNA, completely abolished the cytoprotective effect of PRL against cytokine-induced beta-cell death [4].

Pro-inflammatory cytokines, such as IL-1β, TNF-α and IFN-γ induce the generation of reactive oxygen species (ROS) and reactive nitrogen species (RNS) in pancreatic beta-cells, ultimately leading to beta-cell death [5,6]. They also regulate the expression and/or activity of antioxidant enzymes such as manganese superoxide dismutase (MnSOD) and, to a lower extent, catalase, of transcription factors, such as signal transducer and activator of transcription 1 (STAT1) and nuclear factor kappa B (NF-κB) and key executors of the apoptotic pathway, such as caspase-3 [6–8].

Interestingly, the overexpression of sHSP in tumour models is known to enhance the survival of mammalian cells exposed to cytotoxic stimuli such as heat [9], oxidative stress [10,11], anti-cancerous drugs [10,12], or TNF-α [13,14]. It has already been shown that the protection of lung transplants by HSPB1 against chronic rejection is based on inhibiting apoptosis and defending the cytoskeleton against destruction, protecting the blood vessels, and modulating antioxidant genes [15]. In addition, highly phosphorylated HSPB1 has been reported to interact with a particular protein target: the first enzyme of the pentose phosphate pathway, glucose-6-phosphate dehydrogenase (G6PD) [16], whose activity was also reported to be modulated by HSPB1 expression level [17,18]. This enzyme represents the key enzyme of this major reducing pathway through its ability to transform $NADP^+$ into NADPH leading to the reduction of oxidized glutathione [19]. Moreover, this induces the detoxification of reactive oxygen species and promotes resistance to oxidative stress [20], a phenomenon already described to be linked to HSPB1 and HSPB5 expression in other cell models [17,21–23]. It has also been shown that HSPB1 expression was significantly increased in the hippocampus of diabetic animals and that this occurred in parallel with an increased iNOS and superoxide dismutase (SOD) expression/activity, and enhanced nitrotyrosine and malondialdehyde (MDA) contents [24]. Moreover, since SOD and HSPB1 were expressed in the same cells, the authors suggested that the upregulation of HSPB1 might represent a protective mechanism against diabetes-induced oxidative stress and neuronal death.

Even though it is well described that oxidative stress is directly implicated in beta-cell death, currently there is no data showing a restorative effect of PRL on the redox homeostasis of beta-cells and whether HSPB1 would be related to it. Since islet quality is essential for successful islet transplantation, understanding the mechanisms of beta-cell protection by HSPB1 is of crucial importance for future protection strategies. This knowledge might help to develop alternative strategies to induce the cytoprotective effects of HSPB1 in insulin-producing cells without the undesired side effects of PRL. This could be based on the specific induction of HSPB1, as reported by Gan and collaborators [25] or on the use of short specific peptides presenting the capacity aggravating the protective action of HSPB1 [26]. In view of all the arguments stated above, we set out to analyse whether PRL and/or HSPB1 would display a protective function against oxidative stress in insulin-producing cells.

2. Materials and methods

2.1. MIN6 cell culture

Mouse insulinoma-derived MIN6 cells [27] were maintained in RPMI medium (Life Technologies, Darmstadt, Germany) supplemented with 10% FCS, 100 units/mL ampicillin, 100 µg/mL streptomycin and 10 mM HEPES (Sigma-Aldrich, Munich, Germany). MIN6 cells silenced for HSPB1 (MIN6-shHSPB1) or expressing a control scramble shRNA (MIN6-Sc) were generated and selected with puromycin in our lab [4] and cultured as MIN6 cells.

2.2. Cell treatments

Cells were seeded at different concentrations depending on further experimentation and allowed to attach for a period of 24 h. Treatments with a cocktail of pro-inflammatory cytokines (IL-1β, 0.8 ng/mL; TNF-α, 8 ng/mL; IFN-γ, 4 ng/mL) were carried on for 6 h. Treatments with H_2O_2 (0–100 µM; Merck, Darmstadt, Germany) or menadione (0–20 µM, Sigma-Aldrich) were performed in Krebs-Ringer solution for 2 h. Cells were Incubated with D-alanine (0–20 mM, Sigma-Aldrich) for 24 h in RPMI medium supplemented with the respective D-alanine concentration. PRL (300 ng/mL; Peprotech, Mexico DF, Mexico) treatments were started 30 min before the addition of either cytokines or oxidative stress inducers and kept through the duration of treatment.

2.3. Western blot

Total cell lysates were prepared from cells plated at a density of 5×10^4 cell/cm^2. Equal amounts of proteins from each extract were solubilized in sample buffer (60 mmol/L Tris-HCl [pH 6.8], 2% SDS, 10% glycerol, 0.01% bromophenol blue) and subjected to SDS-PAGE (10%). Proteins were transferred to PVDF membranes, which were previously blocked and then incubated with the following antibodies: rabbit polyclonal antibody for the detection of the FLAG conjugated DAAO protein (600-401-383), rabbit polyclonal anti-catalase (100–4151), both from Rockland, Limerick, PA, USA; mouse monoclonal anti-HSP27 (ab2790, Abcam, Cambridge, United Kingdom); rabbit polyclonal anti-p62 (P0067, Sigma-Aldrich, USA); mouse monoclonal anti-peroxiredoxin 1 (3G5) (LF-MA0214, AbFrontier, South Korea); CuZnSOD and MnSOD antibodies, both obtained from Dr. M. D. Asayama (Kitakyushu, Japan) and rabbit polyclonal anti-G6PD (ab993, Abcam, Cambridge, United Kingdom). The membranes were then incubated with the appropriate horseradish peroxidase-conjugated secondary antibodies. Enhanced chemiluminescence was performed using the ECL detection system (GE Healthcare, Freiburg, Germany). As a loading control, the membranes were stripped and re-probed with goat polyclonal anti-actin C-11 (sc-1615; Santa Cruz), monoclonal anti-alpha-tubulin clone B-5-1-2 (T5168, from Sigma-Aldrich) or mouse monoclonal anti-GAPDH A3 (sc-137179, Santa Cruz). Quantitative densitometry was carried out using the Chemilux Imager (Intas Science Imaging, Göttingen, Germany) and ImageJ software (National Institutes of Health). The volume density of the chemiluminescent bands was calculated as integrated optical density × mm^2 after background correction.

2.4. Immunoprecipitation

Total extracts of MIN6 cells exposed to cytokines for 6 h in the presence or absence of PRL (1 mg of total cell lysates obtained from 6×10^6 cells) were incubated with 4 µg of mouse monoclonal anti-HSP27 antibody (ab2790, Abcam). Thereafter, the immunocomplexes were captured with protein G sepharose (Sigma-Aldrich) as previously described [1]. The beads were washed three times with lysis buffer, boiled for 10 min in sample buffer and subjected to SDS–PAGE. Proteins were either electroblotted onto PVDF membranes or excised from the gels, cut into smaller pieces and transferred to low protein binding polypropylene tubes (Eppendorf, Hamburg, Germany).

2.5. Nano LC-MS/MS analysis

Peptides were obtained from in-gel digestion as previously

described [28]. Gel slices were washed three times for 15 min each with acetonitrile (ACN) 50%, 25 mM ammonium bicarbonate (NH_4HCO_3) and dehydrated with ACN 100% for 5 min followed by vacuum centrifugation. Gel slices were rehydrated and subjected to disulphide bond reduction with 10 mM DTT, 100 mM NH_4HCO_3 for 1 h at 56 °C. The free cysteins were alkylated using 55 mM iodoacetamide, 100 mM NH_4HCO_3 for 45 min in the dark and then washed twice for 15 min with 100 mM NH_4HCO_3. Gel slices were dehydrated with ACN 100% for 5 min followed by vacuum centrifugation and rehydration in digestion buffer containing Trypsin Gold mass spectrometry grade (Promega, Madison, WI, USA), incubated for 1 h at room temperature and then overnight at 37 °C. The supernatant was transferred to a low protein binding tube and tryptic peptides were extracted from the gel slices using ACN 50%, trifluoroacetic acid (TFA) 5% for 30 min. The peptides were desalted using Zip Tip C18 columns (Millipore, Billerica, MA, USA) according to the manufacturer's instructions.

Peptide samples were resuspended in 0.1% formic acid (FA) before analysis using an EASY-nLC system (Thermo Scientific, Waltham, MA, USA) coupled to LTQ-Orbitrap Velos mass spectrometer (Thermo Scientific). The peptides were loaded on an Acclaim PepMap C18 (Thermo Scientific) trap column (2 cm × 100 µm inner diameter; 5 µm) and separated onto an Acclaim PepMap C18 (15 cm × 75 µm inner diameter; 3 µm) column and separated with a gradient from 100% mobile phase A (0.1% FA) to 34% phase B (0.1% FA, 95% ACN) during 60 min, 34%–95% in 10 min and 5 min at 95% at a constant flow rate of 250 nL/min. The LTQ-Orbitrap Velos was operated in positive ion mode with data-dependent acquisition. The full scan was acquired in the Orbitrap at a resolution of 60,000 FWHM in the 400–1200 m/z mass range. Peptide ions were fragmented by CID MS/MS using a normalized collision energy of 35s. The 20 most abundant peptides were selected for MS/MS and dynamically excluded for 30s. All raw data were accessed in Xcalibur software (Thermo Scientific).

2.6. Database searches and bioinformatics analyses

Raw data were searched using the Proteome Discoverer (Thermo Scientific) platform. Database searches were performed using the SEQUEST algorithm embedded in the program. The search parameters were set to: MS accuracy 10 ppm, MS/MS accuracy 0.5 Da, Trypsin digestion with two missed cleavage allowed, fixed carbamidomethyl modification of cysteine and variable modification of oxidized methionine. The tandem mass spectra from the MS/MS experiments were searched against the Uniprot *Mus musculus* non-redundant database, downloaded April 2016. Proteins and peptides were accepted at FDR less than 1%. Proteins with two peptides were considered for further analyses. The number of identified peptides in the presence or absence of PRL was reported. Protein-protein interaction maps and Gene Ontology biological process analysis were performed using the STRING software (https://string-db.org/).

2.7. Viability assay

Cells were seeded at 20,000 cells per well in 100 µL culture medium on 96-well plates and allowed to attach for 24 h before the respective treatments were carried out. Cell viability was then determined by microplate-based MTT assay (3-(4,5-dimethylthiazol-2-yl)-2,5-diphenyl tetrazolium bromide) (Sigma-Aldrich) [29] performed in quadruplicates.

2.8. D-amino acid oxidase (DAAO) and HSPB1 overexpression

The human HSPB1 cDNA and the cDNA of the cytosolic and mitochondrial variant of the *Rhodotorula gracilis* D-amino acid oxidase (rgDAAO, kind gift from Rajiv R. Ratan, Burke Medical Research Institute, White Plains, NY, USA) were subcloned into the lentiviral expression vector pLVX-IRES-Neo from Clontech (Mountain View, CA, USA). Lentiviral particles were prepared as described before in detail [30]: 4×10^6 293FT cells were transfected by calcium phosphate precipitation with the packaging plasmid pPAX2 (11.25 µg), the envelope plasmid pcDNA-MDG (3.75 µg), and the transfer plasmid pLVX-IRES-Neo with the cDNA of Cyto-DAAO, Mito-DAAO or human HSPB1 (15 µg). After 48 h the virus-containing culture medium was collected and centrifuged for 5 min at 700 × g to remove detached cells and cell debris; then the supernatant was filtered through 0.22-µm filters (Millipore). MIN6 cells were infected with the purified viral supernatant for 5–6 h and thereafter the viral supernatant was replaced by fresh medium. Transduced cells were selected with 500 µg/mL Geneticin (Calbiochem, La Jolla, CA, United States).

2.9. Determination of oxidative stress using dichlorodihydrofluorescein diacetate

For the detection of the overall oxidative stress, 20,000 cells were seeded onto black 96-well plates and cultured for 24 h. Then the cells were pre-incubated with 10 µM dichlorodihydrofluorescein diacetate (DCFDA-H_2; Thermo Scientific) for 40 min at 37 °C. The medium containing the chemical probe was discarded and treatment solutions were added. After incubation for 2 h, plates were analysed at 480/520 nm excitation/emission using the Synergy Mx microplate reader (BioTek, Winooski, VT, USA). Detection of ROS by the use of DCFDA-H_2 is dependent on its oxidation to the stable fluorescent derivative dichlorofluorescein and its subsequent accumulation in the cell. Each experiment was performed in quadruplicates; the data were expressed as the percentage of ROS formation in untreated cells normalized by MTT assay as a correction of potentially different seeded cell densities, as no difference in viability was seen during the time of the experiment.

2.10. Assessment of intramitochondrial superoxide radical generation

Superoxide radical generation within the mitochondria was assessed using MitoSOX Red (Thermo Scientific) [31]. MIN6, MIN6-Sc and MIN6-shHSPB1 cells were seeded at a density of 7×10^5 cells per well of 6-well plates and incubated with the indicated treatments. Thereafter the cells were trypsinized and collected by centrifugation at 700 × *g* for 5 min. Cell pellets were suspended in culture medium containing 5 µM MitoSOX Red and incubated for 30 min at 37 °C. Then the cells were washed with PBS and analysed by flow cytometry (CyFlow ML, Sysmex, Kobe, Japan) using the FL-3 channel. Data were analysed by FlowJo software (Tree Star, Ashland, OR, USA).

2.11. Quantification of GSH and GSSG by LC-MS/MS system

Confluent 100 cm^2 culture dishes of the different MIN6 cell lines (4×10^6 cells/assay) were harvested in 160 µL of PBS and 18 µL of extraction buffer (2% TCA; 1.0 mM DTPA) and 2 µL of internal standard (N-acetyl cysteine, 2.0 µg/mL) were added to the samples. The samples were incubated on ice for 15 min and then vortexed for 45 s and incubated on ice for 15 min again. The pH of samples was adjusted to 2.0 by mixing the sample lysate with 200 µL of mobile phase A (0.75 mM ammonium formate, 0.01% formic acid, 1% methanol) and cellular debris were removed by centrifugation at 5,000 × *g*, 4 °C for 10 min. Supernatants were collected and injected in LC-MS/MS system. GSH and GSSG were quantified by LC-MS/MS as previously described [32] with modifications. The analysis was performed in a 6600 Triple-TOF mass spectrometer (AB Sciex, Framingham, MA, USA) coupled with electrospray ionization source (ESI), operated in positive mode. The post-acquisition MRM-like data used for quantification of GSH $(M-H)^+$ (*m/z* 308.0911 → 179.0462), GSSG $(M-H)^+$ (*m/z* 613.1592 → 355.0741), GSSG $(M-H)^{++}$ (*m/z* 307.0863 → 177.0328) and internal standard NAC (*m/z* 164.0 → 76.0215) were completed with collision energies for each individual transition (22 V, GSH; 32 V, GSSG; 25 V, NAC) and 80 V of DP for all analytes. The source

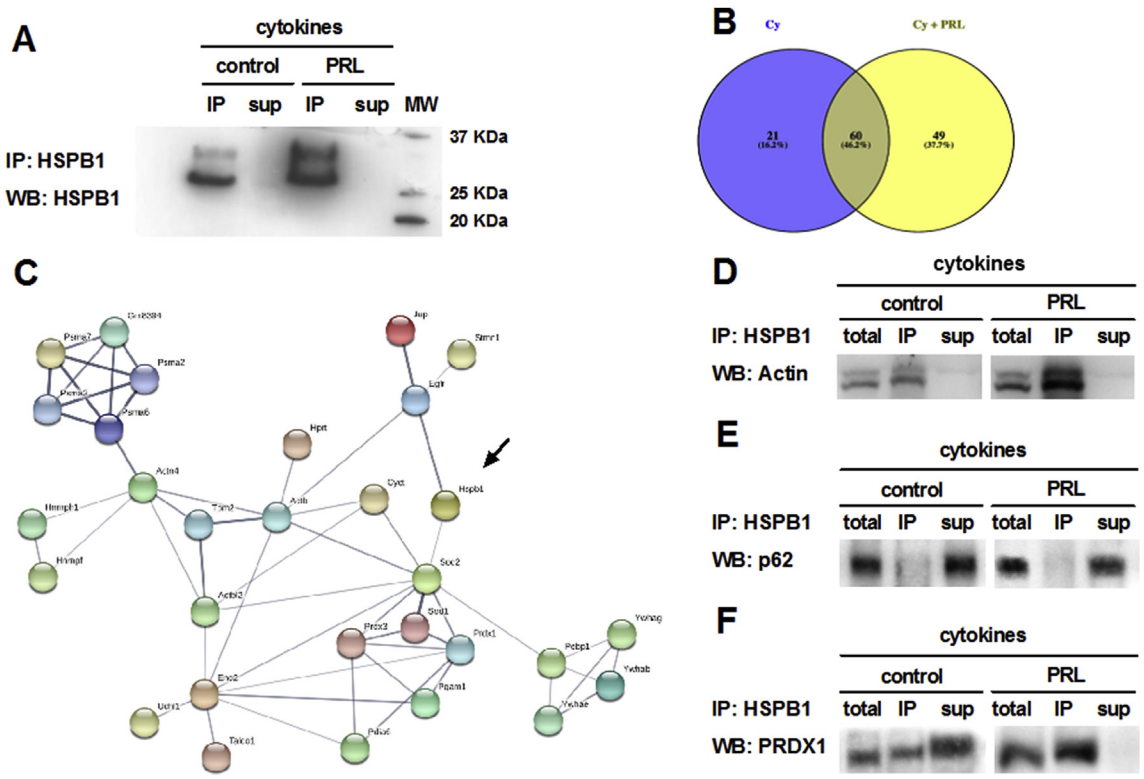

Fig. 1. HSPB1 immunoprecipitation and interacting proteins identification. Total extracts of MIN6 cells exposed to cytokines (IL-1β, 0.8 ng/mL; TNF-α, 8 ng/mL; IFN-γ, 4 ng/mL) for 6 h in the presence or absence of PRL (300 ng/mL) were subjected to immunoprecipitation (IP). (A) Immunoblot of HSPB1 from IP and supernatant (sup). (B) Venn diagram of the distribution of HSPB1-interacting proteins. (C) Interaction map by STRING software of proteins interacting with HSPB1which were found exclusively upon exposure to cytokines and PRL. (D–F) Immunoblots of actin (D), p62 (E) and peroxiredoxin 1 (F) after HSPB1 immunoprecipitation to confirm identification results.

temperature was 450 °C and the spray voltage was set to 5500 V. The chromatographic method was developed in a Nexera UPLC system (Shimadzu, Kyoto, Japan) using a Kinetex C18 analytical column (100 mm × 2.10 mm, 2.6 µm) (Phenomenex, Torrance, CA, USA) eluted with a mobile phase of 0.75 mM ammonium formate/0.01% formic acid/1% methanol (A) and methanol (B) at 0.2 mL/min. Elution was started with 1% B, held for 5 min and followed by a gradient step to 80% from 5 to 6 min. Then, the percentage of B was maintained at 80% for 4 min and was restored to 1% from 10 to 11 min. After this time, the column was equilibrated at 1% B from 11 to 20 min. The column temperature was set at 25 °C and injection volume was 10 µL. With Multiquanti software (3.0, AB Sciex), the concentrations were evaluated by the ratios GSH/NAC and $(GSSG/NAC)_{total}$ plotted against calculated by standard curve.

2.12. Quantification of antioxidant enzyme and glutathione reductase activities

For the quantification of the enzyme activities, 3×10^6 cells were seeded and cultured for 24 h. Then the cells were incubated under control conditions or with 12.5 µM menadione for 2 h. Thereafter whole-cell extracts were prepared in 50 mmol/l potassium phosphate buffer (pH 7.8) through sonication on ice for 1 min in 15 s bursts at 90 W with a Braun-Sonic 125 sonifier (Braun, Melsungen, Germany) and the homogenates were then centrifuged at 10,000 × g at 4 °C for 10 min and stored in aliquots at −20 °C until assayed. Total superoxide dismutase (SOD) activity and the enzyme activities of catalase and glutathione peroxidase (GPx), were quantified as described previously [33]. The activity of glutathione reductase was determined as described by Mannervik [34]. For the calculation of the specific activities the protein content of the cell extracts were determined by the BCA assay (Thermo Scientific).

2.13. Quantification of G6PD activity

The determination of G6PD activity was performed using protein lysates obtained from 5×10^6 MIN6 cells according to Glock and McLean [35], except that iodonitrotetrazolium chloride (INT) was used as electron acceptor as previously described [36]. The 100 µL of reaction medium consisted of 50 mM Tris-HCl buffer pH 7.4, 3.6 mM $MgCl_2$, 1.5 mM glucose-6-phosphate, 0.12 mM nicotinamide adenine dinucleotide phosphate ($NADP^+$), 1.4% Triton X-100, 0.32 mM 1-methoxy phenazine methosulfate (PMS) and 0.2 mM INT. Each experiment was performed in duplicates. Glucose-6-phosphate dehydrogenase reaction medium was incubated at 37 °C for 1 h and read each 2 min at 500 nm in a SpectraMax M2 (Molecular Devices, Sunnyvale, CA, USA) microplate reader.

2.14. Quantification of cellular NADPH/$NADP^+$ content

For the quantification of the cellular $NADP^+$ and NADPH content of the different MIN6 cell lines, 7,500 cells were plated onto white 96-well plates and cultured for 24 h. Thereafter the NADP/NADPH-Glo assay was used and the $NADP^+$ and NADPH content was quantified according to the manufacturer's recommendations (Promega, Madison, WI, USA).

2.15. Statistical analysis

All results were analysed for Gaussian distribution and passed the normality test. The statistical differences between group means were tested by 1- or 2-way Anova when necessary, followed by Bonferroni post-hoc test. A value of $p < 0.05$ was considered statistically

significant. Statistical differences for both ROS production curve fits for exponential growth and EC_{50} curves were calculated by extra-sum-of-squares F test.

3. Results

3.1. HSPB1 interactome in MIN6 cells

In order to better understand the early molecular mechanisms of HSPB1-mediated protection induced by PRL against cytokines and knowing that on the one hand HSPB1 levels started to be significantly induced only after 2 h of hormonal treatment and that on the other hand, caspase-3 and -9 activity peaks occur at 9 h of treatment [4], lysates of MIN6 cells exposed to cytokines for 6 h in the presence or absence of PRL were isolated. HSPB1 was immunoprecipitated (Fig. 1A) and co-immunoprecipitating proteins were then identified by mass spectrometry. The time point of 6 h was specifically chosen in order to maximize the differences between the HSPB1 interactome of the two different situations.

We have described for the first time a specific profile of possible HSPB1-interacting proteins for each condition tested in insulin-producing cells. Of the 130 identified proteins, 60 (46.2%) were detected to interact with HSPB1 under both situations and 21 (16.2%) in the presence of cytokines alone. Nevertheless, when PRL was also present, the number of proteins interacting with HSPB1 was more than twice as high as in the presence of cytokines alone: 49 different proteins (37.7%, Fig. 1B).

Fig. 1C illustrates the interaction map of proteins identified as interacting partners with HSPB1 only when the cells were co-treated with PRL. The map was obtained through the STRING software which links proteins based on available experimental data, taking several techniques and cell models into account. The more lines or the thicker the line connecting two proteins (coloured circles), the more experimental evidence available on their interaction there is (see Fig. S1 for interaction maps of the other treatment conditions).

These results have shown that PRL induces a direct or indirect interaction of HSPB1 with proteins associated to apoptosis inhibition (e.g. cytochrome c, 14-3-3), redox homeostasis (e.g. SOD 1 and 2, peroxiredoxin [PRDX] 1 and 3), carbohydrate metabolism (e.g. malate dehydrogenase) and protein quality control (e.g. several catalytic proteasome subunits, GRP78, ubiquitin-like modifier enzyme), among others (see complete list of identified proteins in Table S1). The HSPB1 interactome results were further confirmed by immunoprecipitation followed by western blotting for a protein that interacts with HSPB1 under both conditions (actin, Fig. 1D), none (p62, Fig. 1E) or only one (PRDX1, Fig. 1F).

3.2. HSPB1 knockdown leads to increased sensibility to oxidative stress

In MIN6 cells co-treated with cytokines and PRL, HSPB1 molecularly interacted with MnSOD and copper zinc SOD (CuZnSOD). These two enzymes catalyse the dismutation of superoxide radicals ($O_2^{\bullet-}$) to molecular oxygen (O_2) and hydrogen peroxide (H_2O_2). Moreover, a specific interaction with peroxiredoxin (PRDX) 1 and 3, both peroxidases defending cells against oxidative damage, was detected [37–40]. Furthermore, many of the proteins identified as interacting with HSPB1 only when MIN6 cells were co-treated with cytokines and PRL, are related to detoxification and cell responses to peroxide and superoxide (Table S2). Therefore, we investigated whether cells knocked down for HSPB1 would show a different sensibility towards oxidative stress. To test this hypothesis MIN6, MIN6-Sc, and MIN6-shHSPB1 cells were incubated with increasing concentrations of menadione, a chemical intramitochondrial ROS generator, and H_2O_2. In fact, MIN6-shHSPB1 cells presented a statistically significant lower EC_{50} of 10.5 and 27.8 μM for menadione and H_2O_2, respectively, which is approximately 20% lower than for both control cell lines (Fig. 2). These results indicated that the presence of HSPB1 is related to an increased resistance of MIN6 cells against oxidative stress-induced toxicity.

We then analysed whether PRL could protect MIN6 cells from loss of viability induced by oxidative stress. Results presented in Fig. 3 indicate not only that PRL is indeed able to protect both control MIN6 cell lines against menadione-induced toxicity (calculated EC_{50} of MIN6 cells: 11.88 and 14.97 μM for control and PRL, respectively, Fig. 3A; calculated EC_{50} of MIN6-Sc cells: 11.10 and 14.74 μM for control and PRL, respectively, Fig. 3B), but also that this effect seems to be mediated by HSPB1, since its silencing completely abrogated PRL's effect on cytoprotection (calculated EC_{50}: 11.61 and 11.91 μM for control and PRL, respectively, Fig. 3C).

3.3. HSPB1 protection is dependent on the subcellular localization of ROS generation

To understand whether the protective effect of HSPB1 is related to specific subcellular production of oxidants, we generated cells expressing cytosolic or mitochondrial variants of the D-amino acid oxidase (DAAO), an enzyme oxidizing D-amino acids to their corresponding imino acids, producing ammonia and hydrogen peroxide as by-products [41]. After confirmation of successful DAAO expression in all cell lines by western blotting (Fig. 4A), the different cell lines where incubated with increasing concentrations of D-alanine and then assessed for cell viability. As expected, the viability of control cells was not significantly affected by D-alanine supplementation to the medium in any of the three cell lines (Fig. 4B). The EC_{50} of MIN6-shHSPB1 cells expressing the cytosolic variant of DAAO was 15% lower than that of the control cells (MIN6: 6.11 mM, MIN6-Sc: 6.18 mM, MIN6-shHSPB1: 5.22 mM, Fig. 4C). When looking at cells expressing the mitochondrial variant of DAAO, the decrease of the EC_{50} of MIN6-shHSPB1 cells was even bigger than that of control cells, of around 40% (MIN6: 5.30 mM, MIN6-Sc: 5.14 mM, MIN6-shHSPB1: 3.21 mM, Fig. 4D), suggesting that HSPB1 is important for the protection against ROS produced in mitochondria, but less against those produced in the cytosol.

3.4. HSPB1 knockdown leads to an increased oxidative status

To further establish whether HSPB1 protects cells by avoiding accumulation of ROS, we quantified the DCF fluorescence as an indicator of the overall oxidative stress in MIN6, MIN6-Sc and MIN6-shHSPB1 cells. Interestingly, MIN6-shHSPB1 cells displayed a significant increased ROS accumulation after menadione incubation, e.g. at one of the intermediary menadione concentrations used (14 μM), mean DFC fluorescence was 154.15% for MIN6, 156.71% for MIN6-Sc and 214.14% for MIN6-shHSPB1 cells compared with untreated cells (Fig. 5A).

Additionally, selective monitoring of ROS within the mitochondria was performed using mitochondria-targeted hydroethidine (MitoSOX Red). In accordance with DCF results, HSPB1 knockdown cells presented a higher MitoSOX fluorescence signal than control cells, e.g. at one of the intermediary menadione concentrations used (14 μM), mean MitoSOX fluorescence was 363.7% for MIN6, 347.7% for MIN6-Sc and 705.4% for MIN6-shHSPB1 cells compared with untreated cells (Fig. 5B).

3.5. HSPB1 overexpression promotes cell resistance against oxidative stress

To confirm the role of HSPB1 in these cells, we generated another cell line overexpressing human HSPB1 (MIN6-rcHSPB1) and a control cell line containing only the empty vector used for HSPB1 overexpression (MIN6-Vec). After successful confirmation of HSPB1 overexpression by western blotting (Fig. 6A), MIN6, MIN6-Vec and MIN6-rcHSPB1 cells were submitted to increasing concentrations of H_2O_2 and menadione to check if overexpression of HSPB1 presented the opposite effect of its knockdown on cell viability. Indeed, HSPB1 overexpression

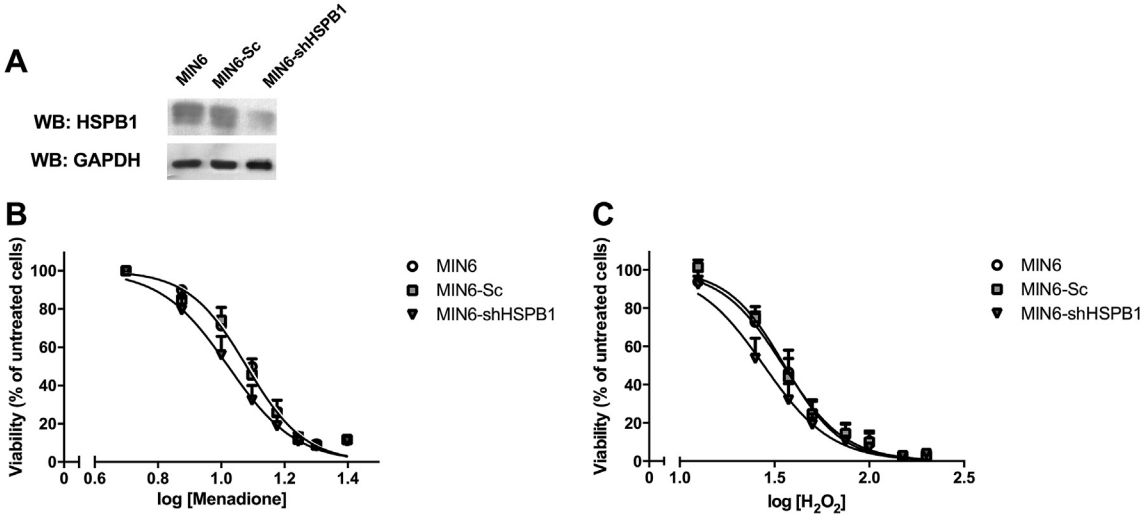

	MIN6	MIN6-Sc	MIN6-shHSPB1
EC_{50} ± SEM (μM)	12.27 ± 1.03	12.02 ± 1.03	10.54 ± 1.04 *
Confidence interval	11.65 to 12.79	11.34 to 12.76	9.786 to 11.31

	MIN6	MIN6-Sc	MIN6-shHSPB1
EC_{50} ± SEM (μM)	35.16 ± 1.04	35.73 ± 1.04	27.80 ± 1.06 *
Confidence interval	30.96 to 39.92	31.95 to 39.92	24.30 to 31.78

Fig. 2. HSPB1 knockdown renders MIN6 cells more sensitive to oxidative stress. HSPB1 expression was confirmed by western blot (WB, A). MIN6, MIN6-Sc, and MIN6-shHSPB1 cells were exposed to increasing concentrations of menadione (0–20 μM, B) or H_2O_2 (0–100 μM, C) for 2 h, then the medium was changed and cells were cultured overnight. Viability was assessed on the following day by MTT assay. Results are shown as means ± SEM; *p < 0.05 compared to control values; n = 6 independent experiments.

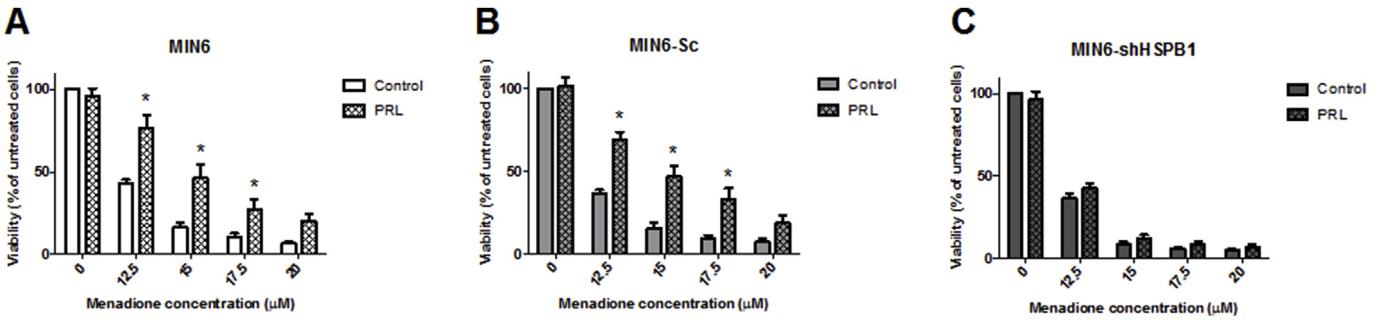

Fig. 3. PRL induces HSPB1-mediated cytoprotection of MIN6 cells against menadione. MIN6 (A), MIN6-Sc (B), and MIN6-shHSPB1 cells (C) were exposed to increasing concentrations of menadione, co-treated or not with PRL (300 ng/mL) for 2 h, then medium was changed and cells were cultured overnight. Viability was assessed on the following day by MTT assay. Results are shown as means ± SEM; *p < 0.05 PRL compared to control of respective treatment; n = 3 independent experiments.

led to a significant increase of the EC_{50} of both menadione (14.5 μM vs. 13.1 μM for control cells, Fig. 6B) and H_2O_2 (32.6 μM vs. 26.2 for control cells, Fig. 6C).

To assess ROS production in HSPB1 overexpressing cells, we analysed the overall oxidative state by DCF fluorescence. Unlike HSPB1 knockdown cells, MIN6-rcHSPB1 cells presented a lower oxidative status, e.g. at one of the intermediary menadione concentrations used (14 μM), mean DCF fluorescence increased to 258.72% in MIN6, 260.93% in MIN6-Vec and 173.10% in MIN6-rcHSPB1 cells compared with untreated cells (Fig. 6D), indicating that accelerated HSPB1 expression resulted in lower oxidant accumulation probably by increasing their antioxidant capacity compared to MIN6 and MIN6-Vec cells.

3.6. Presence of HSPB1 does not change the expression nor the activity of antioxidant enzymes

In order to study possible mechanisms by which HSPB1 is decreasing the levels of oxidants and increasing cell viability, we analysed the expression levels of key antioxidant enzymes. No differences in the expression of CuZnSOD, MnSOD or catalase were observed, regardless of PRL treatment, HSPB1 knockdown or overexpression (Fig. 7). A further possible way of HSPB1 protection could be the direct interaction with one of the antioxidant enzymes thereby increasing its enzyme activity or by stabilizing the enzyme under oxidative conditions and keeping it in its active form. We therefore analysed total SOD enzyme activity as well as the activity of catalase and glutathione peroxidase. Neither under control conditions nor under oxidative stress (12.5 μM menadione for 2 h) changes in enzyme activities could be detected in any of the MIN6 cell lines (Table S3).

3.7. HSPB1 leads to an increase of GSH/GSSG ratio, G6PD activity, and NADPH/$NADP^+$ ratio

When comparing total glutathione levels, no differences could be seen across all MIN6 cell lines analysed (Fig. 8A). However, MIN6-shHSPB1 cells presented a combination of decreased GSH and increased GSSG levels when compared to control MIN6 cells. This resulted in a decrease of the GSH/GSSG ratio by approximately 50% in shHSPB1 cells when compared to the ratio of 5.59 presented by MIN6 cells (Fig. 8B–D). It is important to note that this effect was completely the opposite in HSPB1 overexpressing cells, with a more than 50% increase in GSH/GSSG ratio, accompanied by an increase in GSH and a tendency of a decreased GSSG content, confirming the relevance of HSPB1 to increase the antioxidant capacity of these cells. However, the GSSG

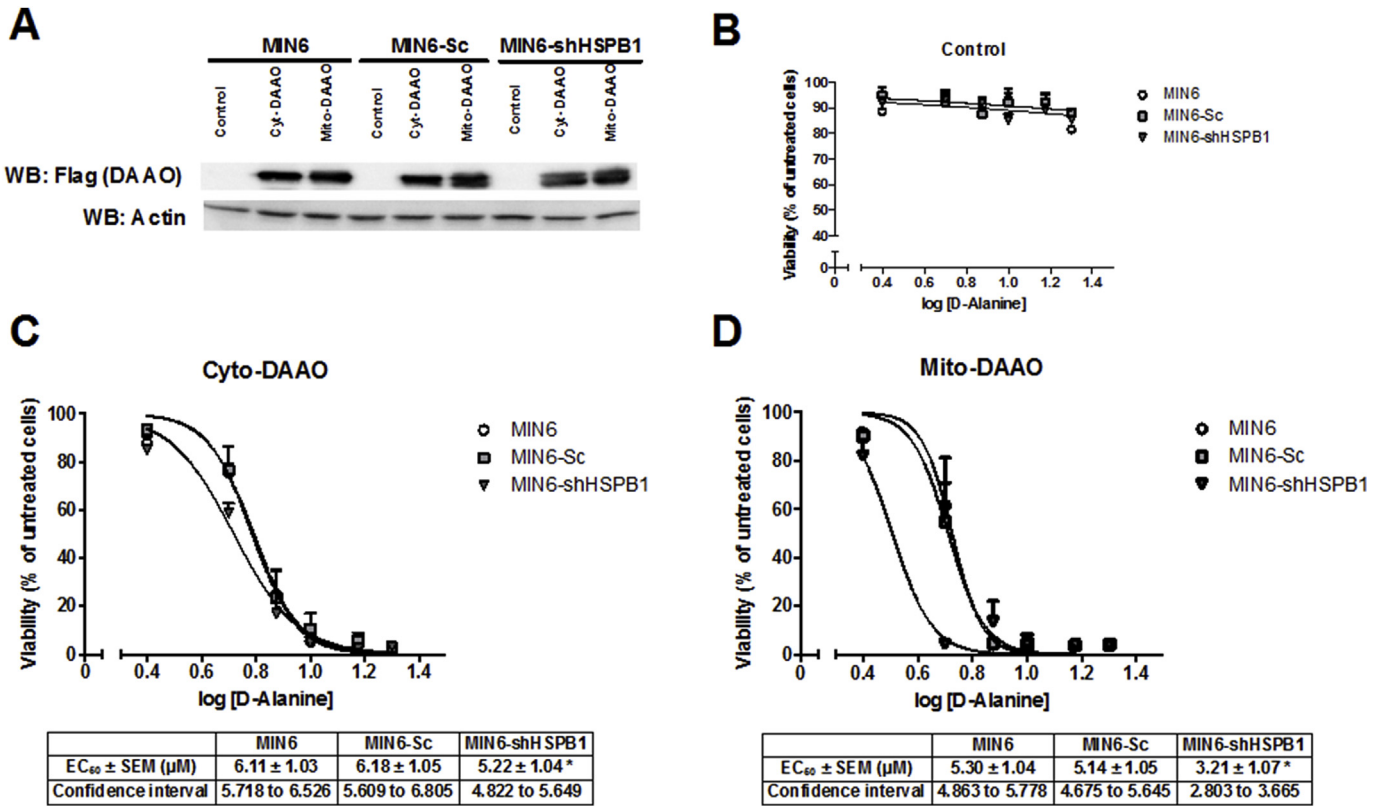

	MIN6	MIN6-Sc	MIN6-shHSPB1
EC_{50} ± SEM (μM)	6.11 ± 1.03	6.18 ± 1.05	5.22 ± 1.04*
Confidence interval	5.718 to 6.526	5.609 to 6.805	4.822 to 5.649

	MIN6	MIN6-Sc	MIN6-shHSPB1
EC_{50} ± SEM (μM)	5.30 ± 1.04	5.14 ± 1.05	3.21 ± 1.07*
Confidence interval	4.863 to 5.778	4.675 to 5.645	2.803 to 3.665

Fig. 4. HSPB1 knockdown in MIN6 cells resulted in a higher sensitivity to H_2O_2 produced in mitochondria, but not in the cytosol. MIN6, MIN6-Sc, and MIN6-shHSPB1 cells expressing DAAO were generated. Expression was confirmed by western blot (WB, A). Control cells (B) or cells expressing the cytosolic (C) or mitochondrial (D) variant of DAAO were exposed to increasing concentrations (0–20 mM) of D-alanine for 24 h. Viability was assessed on the following day by MTT assay. Results are shown as means ± SEM; *p < 0.05 compared to control values; n = 3 independent experiments.

reducing enzyme, glutathione reductase, showed no significant changes in the enzyme activity of the different cell lines, both under control conditions and after oxidative stress (Table S3). Thus, the results presented in this section led us to the conclusion that modifications of the HSPB1 expression resulted in different GSH/GSSG ratios rather than in altered glutathione synthesis rates.

As NADPH is a required cofactor for GSSG reduction by glutathione reductase, we have measured the protein levels of glucose-6-phosphate dehydrogenase (G6PD), the enzyme responsible for the reduction of $NADP^+$ to NADPH, but encountered no differences in any of the studied cell lines (Fig. 9A). However, in comparison to the other cell lines, MIN6-shHSPB1 cells have approximately 40% lower levels of G6PD activity (Fig. 9B). Furthermore, we have also seen a significant decrease in NADPH/$NADP^+$ ratio in HSPB1 knockdown cells of more than 15% when compared to control cells (Fig. 9C). The findings could indicate that the protective effect of HSPB1 is mediated, at least in part, by an increased G6PD activity, leading to a higher NADPH/$NADP^+$ ratio and finally to a higher GSH/GSSG ratio.

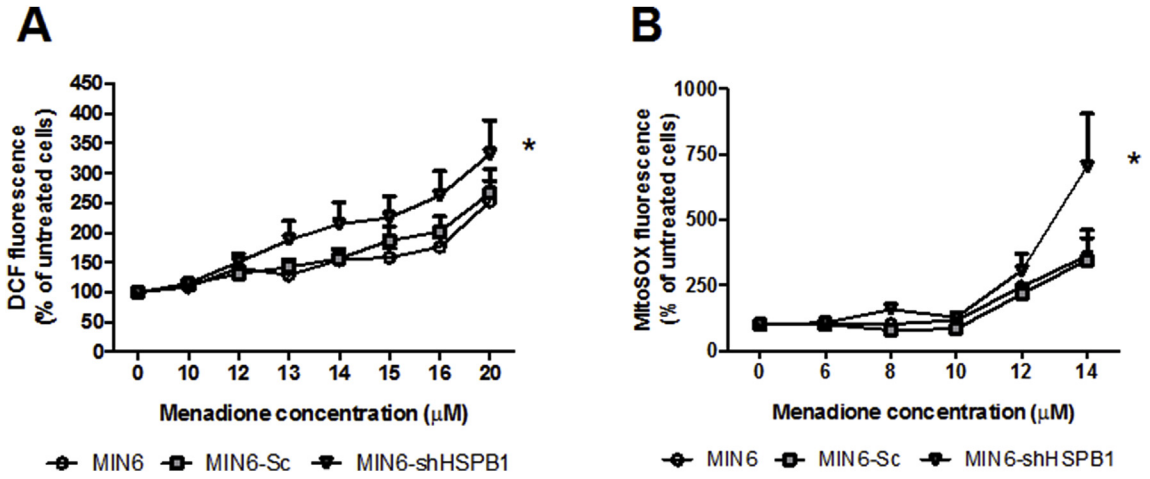

Fig. 5. HSPB1 knockdown led to a redox imbalance towards an oxidant status. MIN6, MIN6-Sc, and MIN6-shHSPB1 cells preincubated with DCFDA-H_2 were exposed to increasing concentrations of menadione for 2 h, and then assessed for fluorescence. MTT assays for normalization were performed immediately thereafter (A). MIN6, MIN6-Sc and MIN6-shHSPB1 cells were exposed to increasing concentrations of menadione for 2 h, incubated with MitoSOX and then assessed for fluorescence by flow cytometry (B). Results are shown as means ± SEM; *p < 0.05 compared to control curves; n = 4 independent experiments.

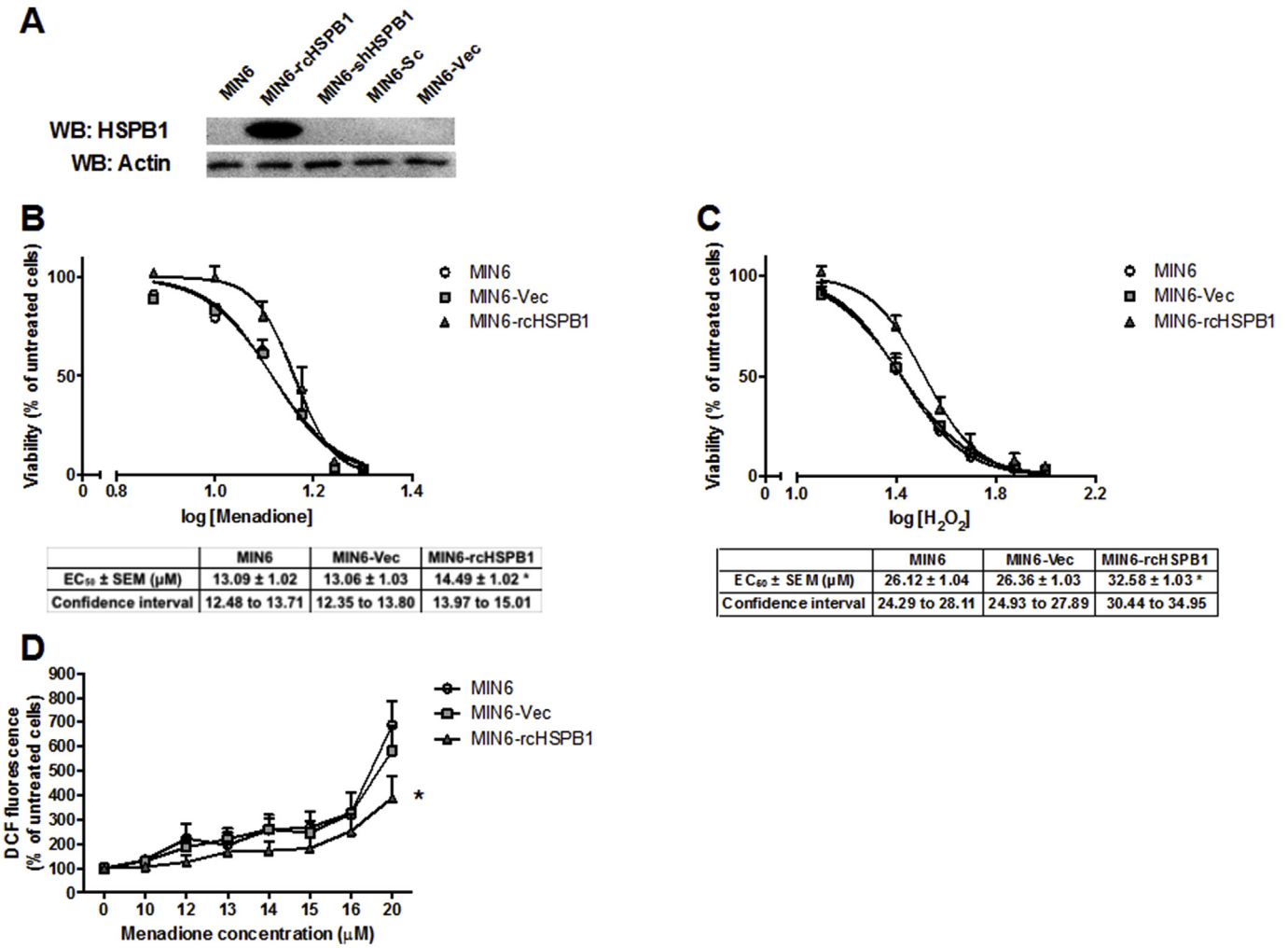

	MIN6	MIN6-Vec	MIN6-rcHSPB1
EC_{50} ± SEM (μM)	13.09 ± 1.02	13.06 ± 1.03	14.49 ± 1.02 *
Confidence interval	12.48 to 13.71	12.35 to 13.80	13.97 to 15.01

	MIN6	MIN6-Vec	MIN6-rcHSPB1
EC_{50} ± SEM (μM)	26.12 ± 1.04	26.36 ± 1.03	32.58 ± 1.03 *
Confidence interval	24.29 to 28.11	24.93 to 27.89	30.44 to 34.95

Fig. 6. HSPB1 overexpression increased cytoprotection against menadione and H_2O_2 and decreased the oxidative status in MIN6 cells. MIN6 cells overexpressing HSPB1 were generated. Expression was confirmed by western blot (WB, A). MIN6, MIN6-Vec, and MIN6-rcHSPB1 cells were exposed to increasing concentrations of menadione (0–20 μM, B) or H_2O_2 (0–100 μM, C) for 2 h, then the medium was changed and cells were cultured overnight. Viability was assessed on the following day by MTT assay. Cells pre-incubated with DCFDA-H_2 were exposed to increasing concentrations of menadione for 2 h, and then the fluorescence was quantified; MTT assays were performed immediately after for normalization (D). Results are shown as means ± SEM; *$p < 0.05$ compared to control values (B,C) or curves (D); $n = 4$ independent experiments.

4. Discussion

Mass spectrometry-based analysis of HSPB1-interactors unveiled that HSPB1 is able to interact with proteins associated with apoptosis inhibition and protein degradation only after PRL treatment has induced its protein level. Although there are no studies on HSPB1-interacting proteins in beta-cells, some of our findings corroborate previous results obtained in other models. It has already been shown in U937 leukaemia cells that HSPB1 overexpression inhibits the cleavage of caspase-9 zymogen, abrogating its activation [42,43]. Moreover, HSPB1 inhibits cytochrome *c*-mediated caspase activation by sequestering both cytochrome *c*, and thus preventing the correct formation/function of the apoptosome complex, and pro-caspase-3 [44]. There is also evidence in other models that HSPB1 is able to improve proteasome stability, allowing an increase in the efficiency of this complex to degrade proteins during endoplasmic reticulum stress by the unfolded protein response [45]. Moreover, a number of proteins, which are already known to participate in maintaining the cellular redox balance, also appear as proteins interacting with HSPB1 only in PRL-exposed MIN6 cells.

Beta-cells are highly metabolically active and extremely dependent on oxidative metabolism for both adenosine triphosphate synthesis and glucose-stimulated insulin secretion [46–48]. This, together with the low expression of antioxidant enzymes and the fact that ROS are an unavoidable by-product of mitochondrial respiration may render beta-cells highly susceptible for damage induced by oxidative stress [49]. In order to further investigate the relationship between PRL treatment, HSPB1 induction and protection against oxidative stress-induced beta-cell death, we have assessed whether PRL could promote an increase in cell viability upon menadione treatment using a cellular model that was previously validated and presented a similar behaviour upon hormonal treatment as already described for primary cultures of human pancreatic islets [2–4]. Indeed, we could see that PRL treatment was able to promote a significant cytoprotection against the mitochondrial oxidative stress inducer menadione, except for cells devoid of HSPB1. Moreover, HSPB1 knockdown in MIN6 beta-cells rendered these cells more susceptible to oxidative stress induced by both menadione and H_2O_2 treatment, showing that this PRL-induced increase in viability is mediated by HSPB1, whose expression is induced in beta-cells by PRL as indicated before [3]. In order to confirm this hypothesis, MIN6 cells overexpressing HSPB1 were generated and, as expected, the overexpression of HSPB1 alone, in the absence of PRL, was able to render MIN6 cells more resistant to oxidative stress induced by menadione and H_2O_2. Interestingly, when the concentration of intracellular oxidants

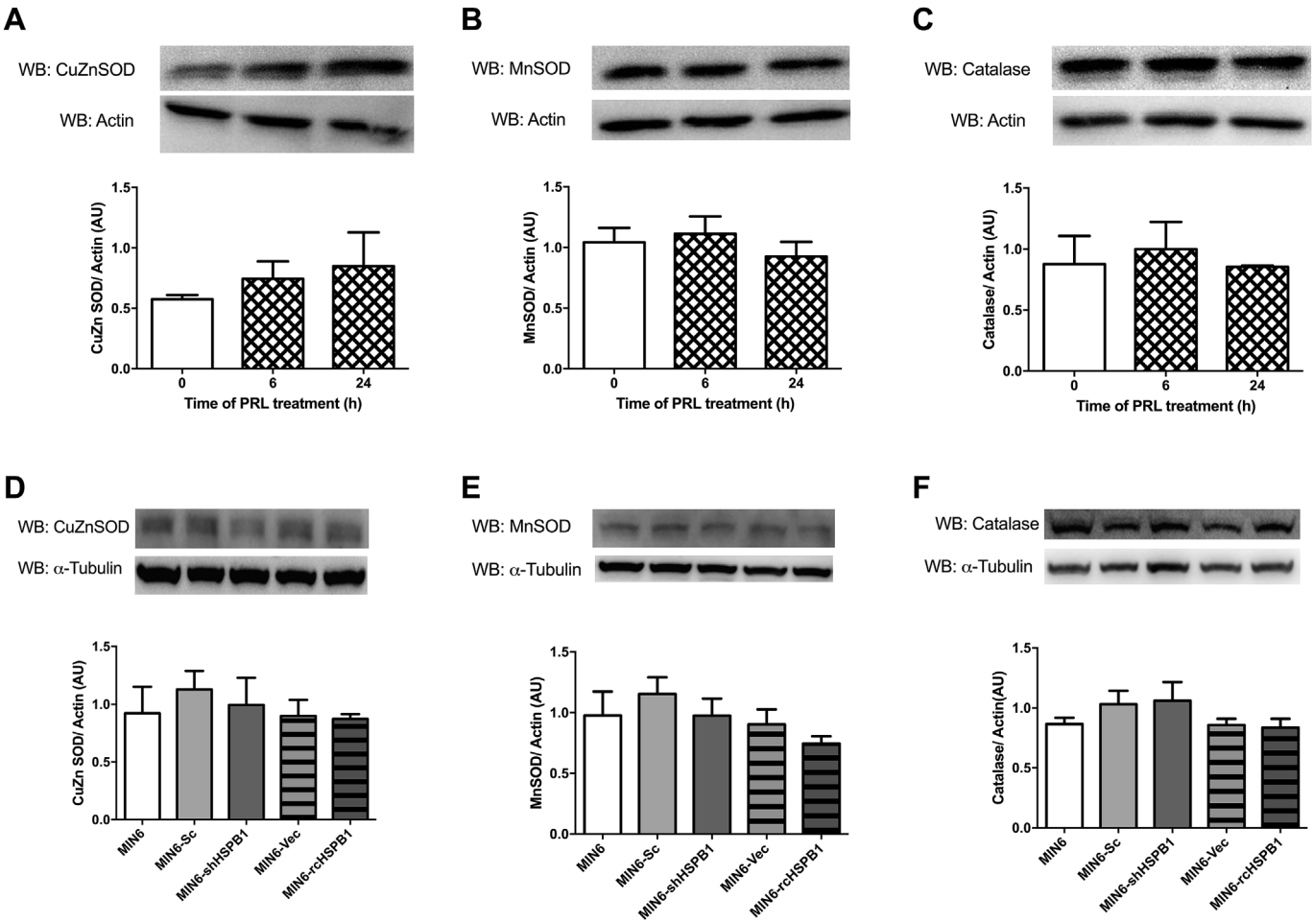

Fig. 7. PRL treatment, HSPB1 silencing or overexpression did not change the expression of antioxidant enzymes. CuZnSOD, MnSOD, and catalase expression was analysed by western blotting, immunoblots shown are representative results and the corresponding histograms are results from densitometry of CuZnSOD (A, D), MnSOD (B, E), and catalase (C, F) in MIN6 cells cultured in the presence or absence of PRL (300 ng/ml) for the indicated times (A–C) or in MIN6, MIN6-Sc, MIN6-shHSPB1, MIN6-Vec and MIN6-rcHSPB1 cells (D–F). Results are shown as means ± SEM; n = 3 independent experiments.

was measured, we could see not only higher ROS-derived fluorescence in shHSPB1-MIN6 cells compared with control cells, but also that MIN6 cells overexpressing HSPB1 displayed the lowest intracellular oxidant levels of all investigated MIN6 cell lines.

It is well known that HSPB1 participates not only in the cellular response to heat shock, but also to oxidative or chemical stress [17,21–23]. However, the contribution of HSPB1 to the antioxidant response remains unclear.

Taking into account that the viability decrease induced by cytosolic ROS generation through the overexpression of cytosolic DAAO in HSPB1 knockdown cells was only 15% lower than that of control cells, while the absence of HSPB1 rendered MIN6 cells significantly more sensitive to the production of oxidants in mitochondria (40% lower viability of HSPB1 knockdown compared to control cells), one can speculate that HSPB1 exerts its cytoprotective role against oxidative stress more strongly in mitochondria.

The increased expression of heat shock proteins (HSP), and especially of HSPB1, has already been shown to protect cells from different cell lines against cell death by interacting with several proteins involved in the mitochondrial apoptosis pathway, as mentioned above. Increased synthesis of HSP is mainly regulated by heat shock factor 1 (HSF1) [50,51]. Indeed, we have already demonstrated that this transcription factor, which is involved in the up-regulation of chaperones, is increased by PRL in beta-cells as well as in pancreatic islets from murine and human origin [4]. One study on kidney cells has revealed that HSF1 disruption decreases HSPB1 protein expression, increases mitochondrial permeability transition pore opening and induces greater mitochondrial membrane potential change [52], suggesting that HSPB1 also exerts effects on the mitochondria itself rather than only on mitochondria-initiated downstream pathways.

Mitochondrial dysfunction has been implicated in the pathogenesis of metabolic diseases, mainly because it is an important source as well as target of ROS. One study reported that oxidative stress precedes the establishment of diabetes and may be the cause of mitochondrial dysfunction that is involved in beta-cell death [53]. In addition, HSPB1 overexpression in L929 cells protected cell morphology and the mitochondrial membrane potential ($\Delta\Psi_m$) after exposure to H_2O_2 [17]. Under normal conditions of culture, higher HSPB1 expression correlated with a higher $\Delta\Psi_m$, and this situation remained identical under conditions of oxidative challenge. The authors also performed cell fractionation to test whether maintenance of $\Delta\Psi_m$ by HSPB1 resulted from an interaction of this chaperone with mitochondrial structures and/or proteins. However, the absence of HSPB1 in the mitochondrial fraction, regardless of exposure or not of the cells to H_2O_2, led the authors to suggest that the $\Delta\Psi_m$ protection conferred by HSPB1 is likely to result from indirect effects rather than from a direct interaction of HSPB1 with mitochondrial structures or proteins. Interestingly, PRDX3, one of the proteins we detected to co-precipitate with HSPB1 only in the presence of PRL, has already been shown to maintain $\Delta\Psi_m$ during cytokine-induced stress [54].

It is important to remember that no differences in the expression levels or the activities of the antioxidant enzymes MnSOD and

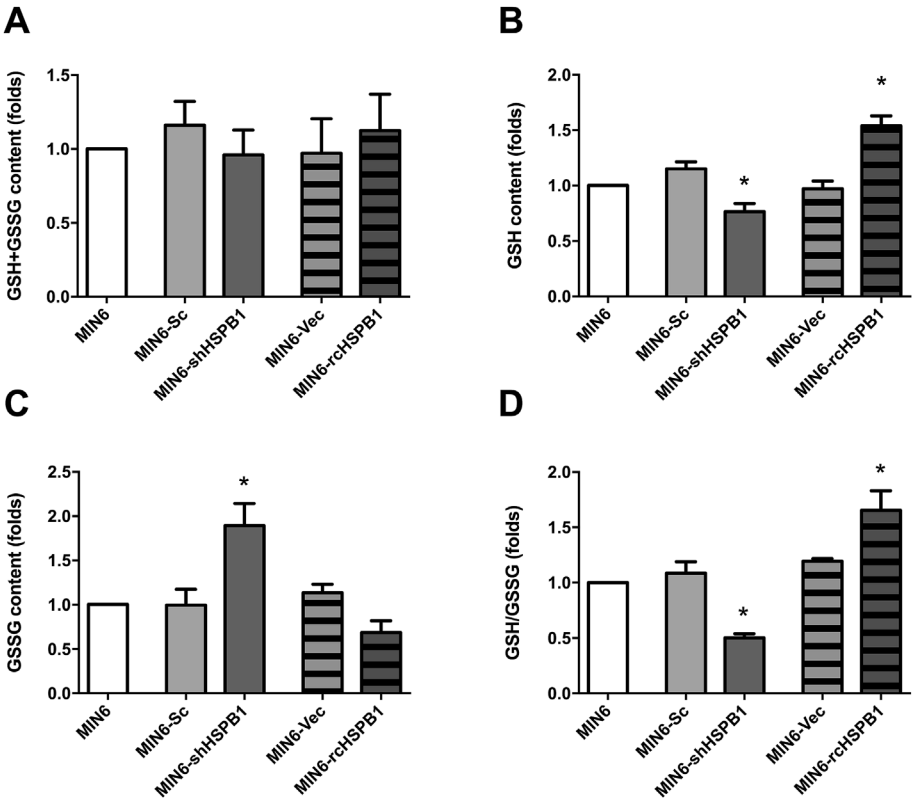

Fig. 8. HSPB1 expression influences the oxidative state of glutathione in MIN6 cells. GSH and GSSG levels were quantified by LC-MS/MS in MIN6, MIN6-Sc, MIN6-shHSPB1, MIN6-Vec, and MIN6-rcHSPB1 cells. Results of total glutathione content (A), GSH (B) and GSSG (C) concentrations were normalized by cell count and represented as folds of MIN6 levels. GSH/GSSG ratios are represented as folds of MIN6 levels (D). Results are shown as means ± SEM; *p < 0.05 compared to control; n = 3 independent experiments.

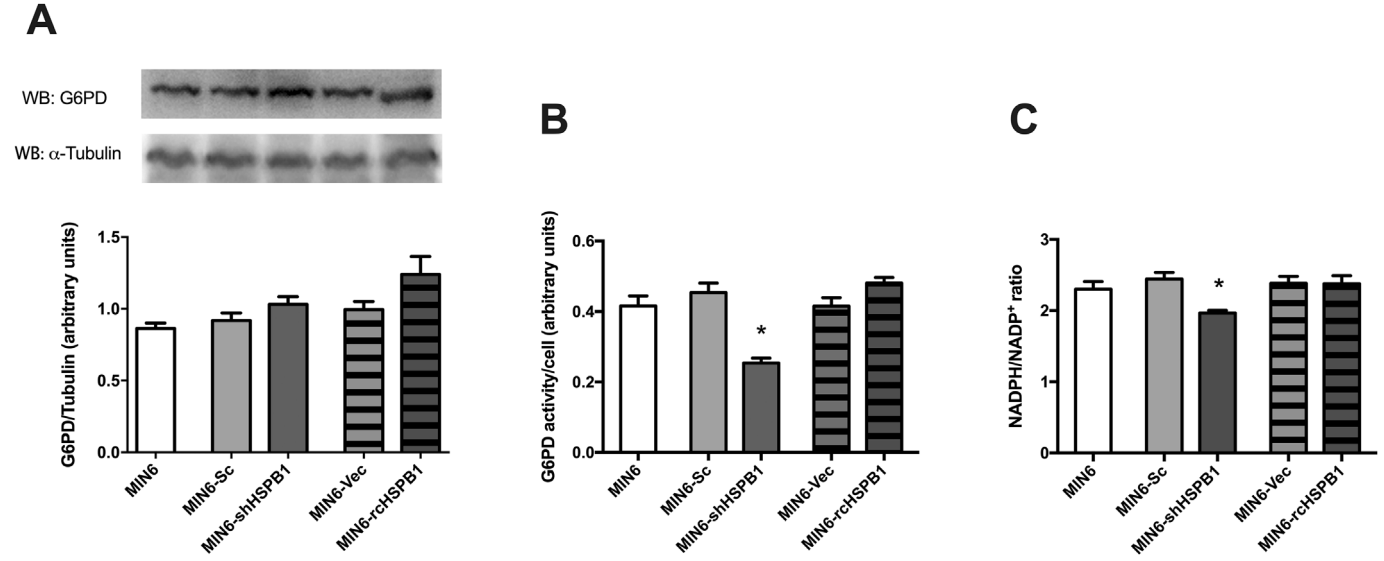

Fig. 9. G6PD activity and NADPH/$NADP^+$ ratio are decreased in HSPB1 knockdown cells. MIN6, MIN6-Sc, MIN6-shHSPB1, MIN6-Vec, and MIN6-rcHSPB1 cells were analysed. Expression of G6PD was assessed by western blot (A), G6PD activity was normalized by cell count (n = 3 independent experiments) (B) and NADPH/$NADP^+$ results are represented as ratios (n = 10 independent experiments) (C). Results are shown as means ± SEM; *p < 0.05 compared to control.

CuZnSOD in any tested MIN6 cell line or after any treatment were observed in the present study. Although data on SOD and HSPB1 interaction has not been reported in beta-cells, in amyotrophic lateral sclerosis (ALS) models HSPB1 interacts with CuZnSOD preventing it from forming large cytotoxic aggregates [55]. However, our results could not seem to follow this latter hypothesis. Furthermore, HSP70, which was also found to interact with HSPB1 in MIN6 cells in the present study, inhibited the aggregation of CuZnSOD in ALS models and prevented its inactivation, leading to an increased cytoprotection [56].

The previously mentioned study on L929 cells also analysed the rate of H_2O_2 consumption in control and HSPB1 overexpressing cells. They found no differences between the cell lines, which indicates that HSPB1 expression does not modify the basic detoxifying abilities of these cells, hence suggesting that catalase activity is not modified by the constitutive expression of HSPB1 [17]. Accordingly, we have not detected a significant difference in catalase expression or activity between control, HSPB1 knocked down or HSPB1 overexpressing MIN6 cells.

During oxidative stress in murine L929 fibrosarcoma cells, HSPB1 increases the pool of GSH [17], which presents reducing and nucleophilic properties, making this compound a key element in cellular protection against oxidative damage to lipids, proteins, and nucleic acids. Furthermore, GSH is a substrate for glutathione transferase and

glutathione peroxidase (GPx), which are responsible for detoxification of xenobiotics and peroxides, respectively [57]. The degradation of peroxides implies that GSH is oxidized to GSSG. The reduction of this latter compound to GSH is catalysed by glutathione reductase (GSR), which uses NADPH as reducing cofactor. The regeneration of oxidized $NADP^+$ to NADPH is part of the pentose phosphate pathway catalysed by the key enzyme G6PD.

Interestingly unlike to what has already been reported in L929 cells, HSPB1 overexpression has not enhanced neither G6PD nor GSR activities in insulin-producing MIN6 cells [17]. Furthermore, HSPB1 was also reported to activate G6PD in response to oxidative stress or DNA damage in glioma cells, where HSPB1 enhances the binding between G6PD and NAD^+-dependent deacetylase sirtuin-2, leading to deacetylation and activation of G6PD [58]. The present study also confirmed that HSPB1 knockdown decreases, while HSPB1 overexpression increases both GSH content and GSH/GSSG ratio. Moreover, HSPB1 silencing also led to increased GSSG levels, presumably caused by decreased G6PD activity and a lowered NADPH/$NADP^+$ ratio.

Thus, the observed HSPB1-mediated cytoprotection of MIN6 cells exposed to either menadione or H_2O_2 could be exerted, at least in part, by an increase in GSH levels and/or activation of G6PD. Since G6PD is cytosolic, this could either reveal the high ROS susceptibility of mitochondria as shown earlier [59] or that GSH support of mitochondria is crucial for resistance against oxidative stress and beta-cell survival.

Altogether these data contributed to confirm that HSPB1 plays an important role in the cytoprotection of MIN6 cells against oxidative stress, which could be mediated by a higher GSH/GSSG ratio rather than by altered glutathione synthesis rates. Since it is well known that this tripeptide is involved in several pathways related with maintenance of redox homeostasis and thus with cell viability, our study also underscores the relevance of pursuing more studies aiming to unveil other different detoxification pathways involved with HSPB1 protective effect. It is important to highlight that understanding the role of HSPB1 on beta-cell cytoprotection may establish the basis of other future clinical approaches leading to the increase of HSPB1 protein levels or to an increased protective activity [25,26], which should avoid the undesired side effects of PRL. Collectively, our results could lead to the mitigation of beta-cell death through the up-regulation of an endogenous protective pathway. Finally, since the number of viable beta-cells during pre-transplant culture significantly correlates with the success of islet transplantation, the cytoprotective properties of HSPB1 described herein may contribute to the development of strategies to increase preservation of viable beta-cells during pre-transplant culture, thus improving the clinical outcome of islet transplantation.

Acknowledgments

The authors would like to thank Martin Wirth and Maren Böger for technical assistance. This work was funded by the Research Training Group 1947 (BioX) of the Deutsche Forschungsgemeinschaft (DFG, Germany), European Foundation for the Study of Diabetes (EFSD, Germany), CNPq, Brazil [grant numbers 441878/2014-8, 151244/2018-9] and FAPESP, Brazil [grant numbers 2013/07029-4, 2017/03618-6, 2013/13914-0, 2016/02881-2, 2014/02745-6, 2016/04676-7 and 2014/17974-0]. The funding sources were not involved in study design; in the collection, analysis and interpretation of data; in the writing of the report; and in the decision to submit the article for publication. Biomass facility at CEFAP-USP is acknowledged for providing access to the MS equipment.

Appendix A. Supplementary data

Supplementary data to this article can be found online at https://doi.org/10.1016/j.freeradbiomed.2019.01.023.

Author contribution

LFT, SL and LL contributed to the conception and experimental design of the study, data analysis, interpretation of the results and wrote the manuscript. LFT performed most of the experiments. RAMW and VMG performed some western blot experiments. AFS acquired and helped in the analysis of the G6PD data. RPS acquired the GSH data. AL constructed and established the DAAO expressing plasmids and helped in the design and analysis of the DAAO experiments. GP performed the MS peptide analysis. FCM helped in the design, analysis and interpretation of the GSH data. WRT helped in the design, analysis and interpretation of the G6PD data. All authors revised the work and approved the final version of the paper.

References

[1] L. Labriola, W.R. Montor, K. Krogh, F.H. Lojudice, T. Genzini, A.C. Goldberg, F.G. Eliaschewitz, M.C. Sogayar, Beneficial effects of prolactin and laminin on human pancreatic islet-cell cultures, Mol. Cell. Endocrinol. 263 (2007) 120–133.
[2] L.F. Terra, M.H. Garay-Malpartida, R.A.M. Wailemann, M.C. Sogayar, L. Labriola, Recombinant human prolactin promotes human beta cell survival via inhibition of extrinsic and intrinsic apoptosis pathways, Diabetologia 54 (2011) 1388–1397.
[3] L. Labriola, G.B. Ferreira, W.R. Montor, M.A.A. Demasi, D.C. Pimenta, F.H. Lojudice, T. Genzini, A.C. Goldberg, F.G. Eliaschewitz, M.C. Sogayar, Prolactin-induced changes in protein expression in human pancreatic islets, Mol. Cell. Endocrinol. 264 (2007) 16–27.
[4] R.A. Wailemann, L.F. Terra, T.C. Oliveira, A.F. Dos Santos, V.M. Gomes, L. Labriola, Heat shock protein B1 is required for the prolactin-induced cytoprotective effects on pancreatic islets, Mol. Cell. Endocrinol. 477 (2018) 39–47, https://doi.org/10.1016/j.mce.2018.05.013.
[5] S. Lenzen, Oxidative stress: the vulnerable beta-cell, Biochem. Soc. Trans. 36 (2008) 343–347.
[6] K.L.A. Souza, E. Gurgul-Convey, M. Elsner, S. Lenzen, Interaction between pro-inflammatory and anti-inflammatory cytokines in insulin-producing cells, J. Endocrinol. 197 (2008) 139–150.
[7] F. Moore, N. Naamane, M.L. Colli, T. Bouckenooghe, F. Ortis, E.N. Gurzov, M. Igoillo-Esteve, C. Mathieu, G. Bontempi, T. Thykjaer, T.F. Ørntoft, D.L. Eizirik, STAT1 is a master regulator of pancreatic {beta}-cell apoptosis and islet inflammation, J. Biol. Chem. 286 (2011) 929–941.
[8] F. Ortis, N. Naamane, D. Flamez, L. Ladrière, F. Moore, D.A. Cunha, M.L. Colli, T. Thykjaer, K. Thorsen, T.F. Orntoft, D.L. Eizirik, Cytokines interleukin-1beta and tumor necrosis factor-alpha regulate different transcriptional and alternative splicing networks in primary beta-cells, Diabetes 59 (2010) 358–374.
[9] J. Landry, P. Chretien, H. Lambert, E. Hickey, L.A. Weber, Heat shock resistance conferred by expression of the human HSP27 gene in rodent cells, J. Cell Biol. 109 (1989) 7–15.
[10] J. Huot, G. Roy, H. Lambert, P. Chrétien, J. Landry, Increased survival after treatments with anticancer agents of Chinese hamster cells expressing the human Mr 27,000 heat shock protein, Cancer Res. 51 (1991) 5245–5252.
[11] P. Mehlen, J. Briolay, L. Smith, C. Diaz-latoud, N. Fabre, D. Pauli, A.P. Arrigo, Analysis of the resistance to heat and hydrogen peroxide stresses in COS cells transiently expressing wild type or deletion mutants of the Drosophila 27-kDa heat-shock protein, Eur. J. Biochem. 215 (1993) 277–284.
[12] C. Garrido, P. Ottavi, A. Fromentin, A. Hammann, A.P. Arrigo, B. Chauffert, P. Mehlen, HSP27 as a mediator of confluence-dependent resistance to cell death induced by anticancer drugs, Cancer Res. 57 (1997) 2661–2667.
[13] P. Mehlen, X. Preville, P. Chareyron, J. Briolay, R. Klemenz, A.P. Arrigo, Constitutive expression of human hsp27, Drosophila hsp27, or human alpha B-crystallin confers resistance to TNF- and oxidative stress-induced cytotoxicity in stably transfected murine L929 fibroblasts, J. Immunol. 154 (1995) 363–374.
[14] P. Mehlen, A. Mehlen, D. Guillet, X. Preville, A.P. Arrigo, Tumor necrosis factor-alpha induces changes in the phosphorylation, cellular localization, and oligomerization of human hsp27, a stress protein that confers cellular resistance to this cytokine, J. Cell. Biochem. 58 (1995) 248–259.
[15] N. Santana-Rodríguez, R. García-Herrera, B. Clavo, P. Llontop, M.A. Ponce-González, J. Villar, A. López-García, M.D. Fiuza, J.C. Rodríguez-Bermejo, J.M. García-Castellano, R.P. Machín, J.A. Ruíz-Caballero, Y. Brito, L. Fernández-Pérez, Searching for novel molecular targets of chronic rejection in an orthotopic experimental lung transplantation model, J. Heart Lung Transplant. 31 (2012) 213–221.
[16] C. Cosentino, D. Grieco, V. Costanzo, ATM activates the pentose phosphate pathway promoting anti-oxidant defence and DNA repair, EMBO J. 30 (2011) 546–555.
[17] X. Préville, F. Salvemini, S. Giraud, S. Chaufour, C. Paul, G. Stepien, M. V Ursini, A.P. Arrigo, Mammalian small stress proteins protect against oxidative stress through their ability to increase glucose-6-phosphate dehydrogenase activity and by maintaining optimal cellular detoxifying machinery, Exp. Cell Res. 247 (1999) 61–78.
[18] L.J. Yan, E.S. Christians, L. Liu, X. Xiao, R.S. Sohal, I.J. Benjamin, Mouse heat shock transcription factor 1 deficiency alters cardiac redox homeostasis and increases mitochondrial oxidative damage, EMBO J. 21 (2002) 5164–5172.
[19] W.-Y. Kuo, T.K. Tang, Effects of G6PD overexpression in NIH3T3 cells treated with

tert-butyl hydroperoxide or paraquat, Free Radic. Biol. Med. 24 (1998) 1130–1138.
[20] F. Salvemini, A. Franzé, A. Iervolino, S. Filosa, S. Salzano, M.V. Ursini, Enhanced glutathione levels and oxidoresistance mediated by increased glucose-6-phosphate dehydrogenase expression, J. Biol. Chem. 274 (1999) 2750–2757.
[21] P. Mehlen, C. Kretz-remy, X. Preville, A.P. Arrigo, Human hsp27, Drosophila hsp27 and human alphaB-crystallin expression-mediated increase in glutathione is essential for the protective activity of these proteins against TNFalpha-induced cell death, EMBO J. 15 (1996) 2695–2706.
[22] A.P. Arrigo, Hsp27: novel regulator of intracellular redox state, IUBMB Life 52 (2001) 303–307.
[23] A.P. Arrigo, S. Virot, S. Chaufour, W. Firdaus, C. Kretz-Remy, C. Diaz-Latoud, Hsp27 consolidates intracellular redox homeostasis by upholding glutathione in its reduced form and by decreasing iron intracellular levels., Antioxid, Redox Signal 7 (2005) 414–422.
[24] R. Mastrocola, F. Barutta, S. Pinach, G. Bruno, P.C. Perin, G. Gruden, Hippocampal heat shock protein 25 expression in streptozotocin-induced diabetic mice, Neuroscience 227 (2012) 154–162.
[25] N. Gan, Y.-C. Wu, M. Brunet, C. Garrido, F.-L. Chung, C. Dai, L. Mi, Sulforaphane activates heat shock response and enhances proteasome activity through up-regulation of Hsp27, J. Biol. Chem. 285 (2010) 35528–35536.
[26] B. Gibert, S. Simon, V. Dimitrova, C. Diaz-Latoud, A.P. Arrigo, Peptide aptamers: tools to negatively or positively modulate HSPB1(27) function, Philos. Trans. R. Soc. Lond. B Biol. Sci. 368 (2013) 20120075.
[27] H. Ishihara, T. Asano, K. Tsukuda, H. Katagiri, K. Inukai, M. Anai, M. Kikuchi, Y. Yazaki, J.I. Miyazaki, Y. Oka, Pancreatic beta cell line MIN6 exhibits characteristics of glucose metabolism and glucose-stimulated insulin secretion similar to those of normal islets, Diabetologia 36 (1993) 1139–1145.
[28] L.F. Terra, P.C. Teixeira, R.A.M. Wailemann, A. Zelanis, G. Palmisano, E. Cunha-Neto, J. Kalil, M.R. Larsen, L. Labriola, M.C. Sogayar, Proteins differentially expressed in human beta-cells-enriched pancreatic islet cultures and human insulinomas, Mol. Cell. Endocrinol. 381 (2013) 16–25.
[29] T. Mosmann, Rapid colorimetric assay for cellular growth and survival: application to proliferation and cytotoxicity assays, J. Immunol. Methods 65 (1983) 55–63.
[30] R. Zufferey, T. Dull, R.J. Mandel, A. Bukovsky, D. Quiroz, L. Naldini, D. Trono, Self-inactivating lentivirus vector for safe and efficient in vivo gene delivery, J. Virol. 72 (1998) 9873–9880.
[31] K.M. Robinson, M.S. Janes, M. Pehar, J.S. Monette, M.F. Ross, T.M. Hagen, M.P. Murphy, J.S. Beckman, Selective fluorescent imaging of superoxide in vivo using ethidium-based probes, Proc. Natl. Acad. Sci. U. S. A. 103 (2006) 15038–15043.
[32] D. Carroll, D. Howard, H. Zhu, C.M. Paumi, M. Vore, S. Bondada, Y. Liang, C. Wang, D.K. St Clair, Simultaneous quantitation of oxidized and reduced glutathione via LC-MS/MS: an insight into the redox state of hematopoietic stem cells, Free Radic. Biol. Med. 97 (2016) 85–94.
[33] M. Tiedge, S. Lortz, R. Munday, S. Lenzen, Complementary action of antioxidant enzymes in the protection of bioengineered insulin-producing RINm5F cells against the toxicity of reactive oxygen species, Diabetes 47 (1998) 1578–1585.
[34] B. Mannervik, Measurement of Glutathione Reductase Activity, Curr. Protoc. Toxicol., Chapter 7.2, Unit 7.2.1- 7.2.4 (2001).
[35] G.E. Glock, P. McLean, Further studies on the properties and assay of glucose 6-phosphate dehydrogenase and 6-phosphogluconate dehydrogenase of rat liver, Biochem. J. 55 (1953) 400–408.
[36] C.D. Santos, W.R. Terra, Plasma membrane-associated amylase and trypsin: intracellular distribution of digestive enzymes in the midgut of the cassava hornworm, Erinnyis ello, Insect Biochem. 14 (1984) 587–594.
[37] W. Lee, T. Wells, M. Kantorow, Localization and H2O2-specific induction of PRDX3 in the eye lens, Mol. Vis. 13 (2007) 1469–1474.
[38] S. De Simoni, J. Goemaere, B. Knoops, Silencing of peroxiredoxin 3 and peroxiredoxin 5 reveals the role of mitochondrial peroxiredoxins in the protection of human neuroblastoma SH-SY5Y cells toward MPP+, Neurosci. Lett. 433 (2008) 219–224.
[39] M. Shiota, H. Izumi, N. Miyamoto, T. Onitsuka, E. Kashiwagi, A. Kidani, G. Hirano, M. Takahashi, M. Ono, M. Kuwano, S. Naito, Y. Sasaguri, K. Kohno, Ets regulates peroxiredoxin1 and 5 expressions through their interaction with the high-mobility group protein B1, Cancer Sci. 99 (2008) 1950–1959.
[40] S.S. Mukhopadhyay, K.S. Leung, M.J. Hicks, P.J. Hastings, H. Youssoufian, S.E. Plon, Defective mitochondrial peroxiredoxin-3 results in sensitivity to oxidative stress in Fanconi anemia, J. Cell Biol. 175 (2006) 225–235.
[41] R.E. Haskew-Layton, J.B. Payappilly, N.A. Smirnova, T.C. Ma, K.K. Chan, T.H. Murphy, H. Guo, B. Langley, R. Sultana, D.A. Butterfield, S. Santagata, M.J. Alldred, I.G. Gazaryan, G.W. Bell, S.D. Ginsberg, R.R. Ratan, Controlled enzymatic production of astrocytic hydrogen peroxide protects neurons from oxidative stress via an Nrf2-independent pathway, Proc. Natl. Acad. Sci. Unit. States Am. 107 (2010) 17385–17390.
[42] C. Garrido, J.M. Bruey, A. Fromentin, A. Hammann, A.P. Arrigo, E. Solary, HSP27 inhibits cytochrome c-dependent activation of procaspase-9, FASEB J. 13 (1999) 2061–2070.
[43] J.M. Bruey, C. Ducasse, P. Bonniaud, L. Ravagnan, S.A. Susin, C. Diaz-Latoud, S. Gurbuxani, A.P. Arrigo, G. Kroemer, E. Solary, C. Garrido, Hsp27 negatively regulates cell death by interacting with cytochrome c, Nat. Cell Biol. 2 (2000) 645–652.
[44] C.G. Concannon, S. Orrenius, A. Samali, Hsp27 inhibits cytochrome c-mediated caspase activation by sequestering both pro-caspase-3 and cytochrome c, Gene Expr. 9 (2001) 195–201.
[45] A.P. Arrigo, Human small heat shock proteins: protein interactomes of homo- and hetero-oligomeric complexes: an update, FEBS Lett. 587 (2013) 1959–1969.
[46] T.J. Pullen, G.A. Rutter, When less is more: the forbidden fruits of gene repression in the adult β-cell, Diabetes Obes. Metab. 15 (2013) 503–512.
[47] G.A. Rutter, T.J. Pullen, D.J. Hodson, A. Martinez-Sanchez, Pancreatic β-cell identity, glucose sensing and the control of insulin secretion, Biochem. J. 466 (2015) 203–218.
[48] N. Sekine, V. Cirulli, R. Regazzi, L.J. Brown, E. Gine, J. Tamarit-Rodriguez, M. Girotti, S. Marie, M.J. MacDonald, C.B. Wollheim, Low lactate dehydrogenase and high mitochondrial glycerol phosphate dehydrogenase in pancreatic beta-cells. Potential role in nutrient sensing, J. Biol. Chem. 269 (1994) 4895–4902.
[49] P.A. Gerber, G.A. Rutter, The role of oxidative stress and hypoxia in pancreatic beta-cell dysfunction in diabetes mellitus, Antioxidants Redox Signal. 26 (2017) 501–518.
[50] L. Pirkkala, P. Nykänen, L. Sistonen, Roles of the heat shock transcription factors in regulation of the heat shock response and beyond, FASEB J. 15 (2001) 1118–1131.
[51] N.D. Trinklein, W.C. Chen, R.E. Kingston, R.M. Myers, Transcriptional regulation and binding of heat shock factor 1 and heat shock factor 2 to 32 human heat shock genes during thermal stress and differentiation, Cell Stress Chaperones 9 (2004) 21–28.
[52] L.-J. Yan, N.S. Rajasekaran, S. Sathyanarayanan, I.J. Benjamin, Mouse HSF1 disruption perturbs redox state and increases mitochondrial oxidative stress in kidney, Antioxidants Redox Signal. 7 (2005) 465–471.
[53] C. Malaguti, P.G. La Guardia, A.C.R. Leite, D.N. Oliveira, R.L. de Lima Zollner, R.R. Catharino, A.E. Vercesi, H.C.F. Oliveira, Oxidative stress and susceptibility to mitochondrial permeability transition precedes the onset of diabetes in auto-immune non-obese diabetic mice, Free Radic. Res. 48 (2014) 1494–1504.
[54] G. Wolf, N. Aumann, M. Michalska, A. Bast, J. Sonnemann, J.F. Beck, U. Lendeckel, P. Newsholme, R. Walther, Peroxiredoxin III protects pancreatic ß cells from apoptosis, J. Endocrinol. 207 (2010) 163–175.
[55] J.J. Yerbury, D. Gower, L. Vanags, K. Roberts, J.A. Lee, H. Ecroyd, The small heat shock proteins αB-crystallin and Hsp27 suppress SOD1 aggregation in vitro, Cell Stress Chaperones 18 (2013) 251–257.
[56] G.A. Shinder, M.C. Lacourse, S. Minotti, H.D. Durham, Mutant Cu/Zn-superoxide dismutase proteins have altered solubility and interact with heat shock/stress proteins in models of amyotrophic lateral sclerosis, J. Biol. Chem. 276 (2001) 12791–12796.
[57] A. Meister, M.E. Anderson, Glutathione., Annu. Rev. Biochem. 52 (1983) 711–760.
[58] H. Ye, H. Huang, F. Cao, M. Chen, X. Zheng, R. Zhan, HSPB1 Enhances SIRT2-Mediated G6PD Activation and Promotes Glioma Cell Proliferation, PLoS One 11 (2016) e0164285.
[59] I. Mehmeti, E. Gurgul-Convey, S. Lenzen, S. Lortz, Induction of the intrinsic apoptosis pathway in insulin-secreting cells is dependent on oxidative damage of mitochondria but independent of caspase-12 activation, Biochim. Biophys. Acta Mol. Cell Res. 1813 (2011) 1827–1835.